University of Florence
School of Engineering

Master degree program in
Computer Engineering

Disparity coherent stereo video watermarking

Master Thesis of

Benedetta Barbetti, Michaela Servi

December 2015

Supervisor:

Prof. Alessandro Piva

Advisors:

Prof. Carlo Colombo
Dott. Pasquale Ferrara
Dott. Francesca Uccheddu

Academic Year 2014/2015

Abstract

Contents

List of Figures

List of Tables

Introduction

In the last few years the stereoscopic technique has become a great part of image and video processing.

In medical diagnosis and endoscopic surgery as in fault detection in manufactory industry, army and arts, multiview imaging is considered as a key enabler for professional added value services.

Nowdays stereoscopic techniques are also used in people tracking and mobile robotics navigation for economic reasons and to improve performances.

Finally the worldwide success of 3D movie releases and 3D video games and the deployment of 3D televisions made the nonprofessional user aware about a new type of multimedia entertainment experience.

The increasing production and distribution of these contents leads to the concerns over copyright protection.

Digital watermarking can be considered as the most flexible property right protection technology, since it adds some information (a mark, i.e. copyright information) in the original content without altering its visual quality so that such a marked content can be further distributed/consumed by another user without any restriction; still, the legitimate/illegitimate usage can be determined at any moment by detecting the mark. In same case the watermarking protection mechanism, instead of restricting the media copy/distribution/consumption, provides means for tracking the source of

the content illegitimate usage.

The purpose of this thesis is to provide a new watermarking system for copyright protection of stereoscopic videos.

The method operates in the frequency and in the spatial domain by embedding a pseudo-random sequence of real numbers in a selected set of DFT coefficients of the left image; then the reference watermark is distorted according to the depth information prior to insertion and spatially added to the right image.

This new algorithm is robust against view synthesis and lossy compression.

In Chapter **??**...

Chapter 1

Stereoscopic Video

In a wide variety of image processing applications, explicit depth information is required in addition to general image informations, such as intensities, color, densities.
Examples of such applications are found in 3D vision (robot vision, photogrammetry, remote sensing systems), in medical imaging (computer tomography, magnetic resonance imaging, microsurgery), in remote handling of objects (random bin picking), in space exploration (mobile robotics navigation) or 3D movies and videogames.
In each of these cases, depth information is essential for accurate image analysis or for enhancing the realism.
In remote sensing the terrain's elevation needs to be accurately determined for map production, in remote handling an operator needs to have precise knowledge of the threedimensional organization of the area to avoid collisions and misplacements.

Depth in real world scenes can be explicitly measured by a number of range sensing devices such as by laser range sensors, by structured light or

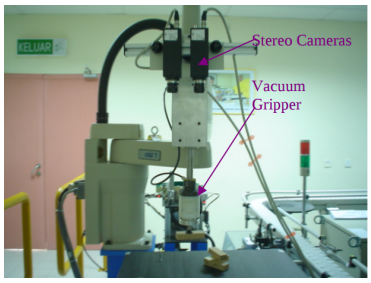

(a) In bin picking applications stereo vision helps to reconstruct the 3D environment and detect the part of the object to be robotically picked

(b) Surgical robot *Da vinci* is provided with a stereoscopic camera that allows a tridimensional view of the operative filed.

Figure 1.1: Stereoscopy in medical and industrial field

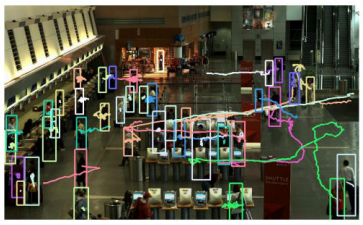

(a) In people tracking application stereo vision improves segmentation thanks to depth information and it's less sensible to light changes.

(b) In mobile robotics navigation stereo vision has became the first choice technology because it provids a lot of quality data for low costs.

Figure 1.2: Stereoscopy application's fields

by ultrasound. However it's usually undesirable to have separate systems for acquiring the intensity and the depth information because of the relative low resolution of the range sensing devices and because it's not an easy task to fuse information from different type of sensors; for these reasons and for a non-negligible economic factor stereoscopic vision has becoming the technology of choice in these type of applications.

(a) Stereo video frames, left and right.

(b) Overlap of the two frames.

(c) 3D view with specific glasses

(d) Polarized glasses for 3D view

Figure 1.3: Stereoscopy in 3D video games

1.1 Stereo vision

In image processing stereo vision is the process of extracting 3D information from multiple 2D views of a scene.

The 3D information can be obtained from a pair of images, also known as a stereo pair, by estimating the relative depth of points in the scene.

From the anatomic point of view, the human brain calculates the depth in a visual scene mainly by processing the information brought by the images seen by the left and the right eyes. These left and right images are slightly different because the eyes have biologically different emplacements.

Consequently, the straightforward way of achieving stereoscopic digital imaging is to emulate the Human Visual System (HSV) by setting-up (under controlled geometric positions), two traditional 2D cameras.

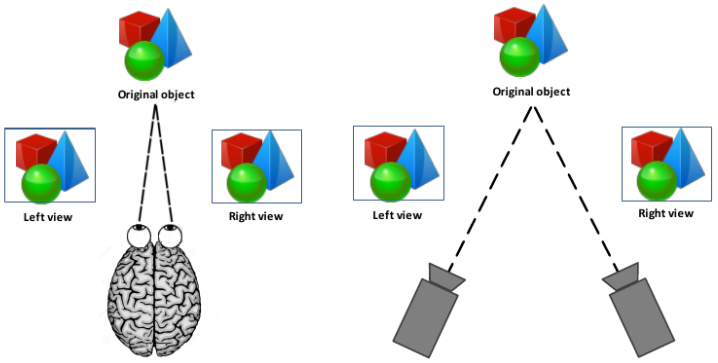

(a) Binocular human visual system (b) Stereoscopic system

Figure 1.4: Binocular human vision vs. stereoscopic content acquisition.

1.1.1 Acquisition of stereoscopic images

In order to be able to perceive depth using recorded images, a stereoscopic camera is required, which consists of two cameras that capture two different, horizontally shifted perspective viewpoints; with two (or more) cameras we can infer depth, by means of triangulation, if we are able to find corresponding points in the two images (Figure 1.5).

The camera setup should be geometrically calibrated such that the two

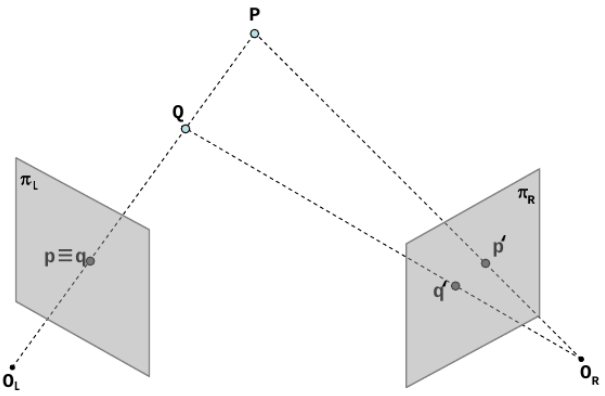

Figure 1.5: Triangulation: with two cameras the depth of

cameras capture the same part of the real world scene.

Calibration of a stereo camera system involves the estimation of the intrinsic and extrinsic parameters of the model: intrinsic parameters embody the characteristics of the optical system and its geometric relationship with the image sensor, extrinsic parameters relate the location and orientation of the second camera with respect to the first one in the 3D space (Figure 1.6).

These parameters can be used to rectify a stereo pair of images to make

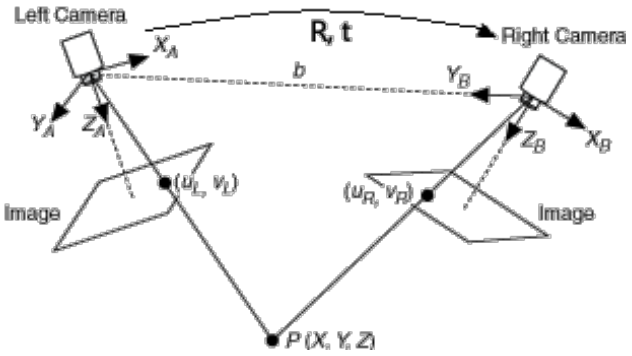

Figure 1.6: Stereo camera model

them appear as the two image planes are parallel (Figure 1.7); once the images are rectified, epipolar geometry it's used to find corresponding points and compute the disparity map.

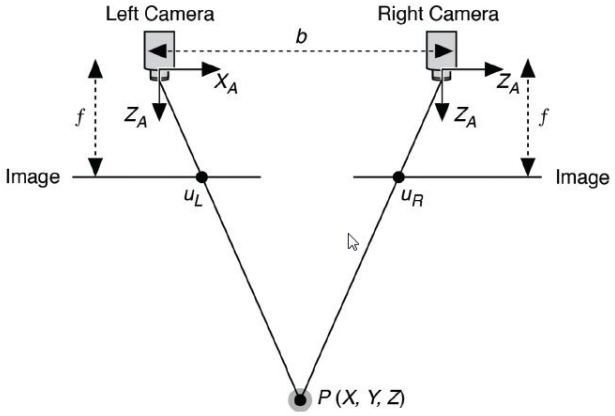

Figure 1.7: Rectified stereo cameras

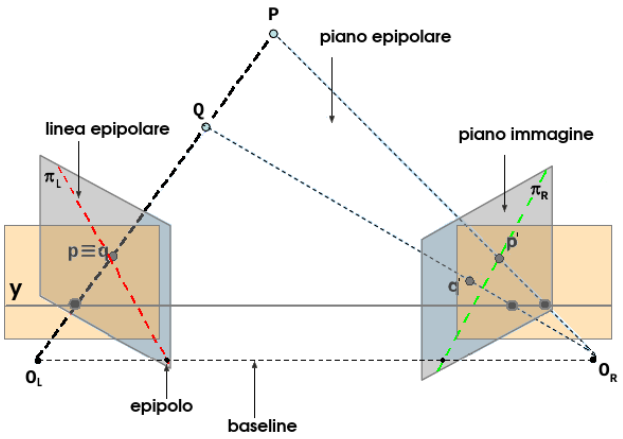

Figure 1.8: Rectified images: corresponding points (p, p'), projection of the same 3D point (P) are constrained on the same image horizontal line, the epipolar line

1.1.2 Disparity map computation

With the stereo rig in standard form and by considering similar triangles in Figure 1.9 (PO_LO_R and Ppp'):

$$\frac{b}{Z} = \frac{(b + x_L) - x_R}{Z - f}$$

so

$$Z = \frac{b \cdot f}{x_L - x_R} = \frac{b \cdot f}{d}$$

where $d = x_L - x_R$ it's called *disparity*.

Disparity is, therefore, the difference between the x coordinates of two corresponding points and it is usually encoded with greyscale image (Figure 1.10c), where points closer to the cameras are brighter and correspond to a higher disparity.

In order to compute the disparity map is necessary to find corresponding points; stereo correspondance is though a challenging task that has to manage with perspective distortions, uniform and ambiguous regions, repetitive patterns, occlusions and discontinuities(Figure 1.11).

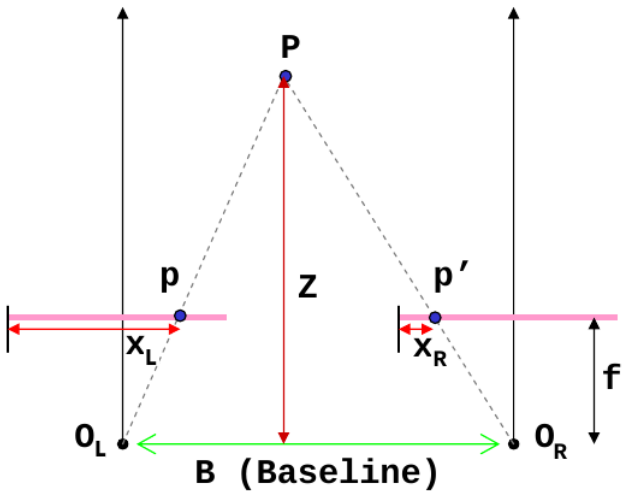

Figure 1.9: Geometry of standard form

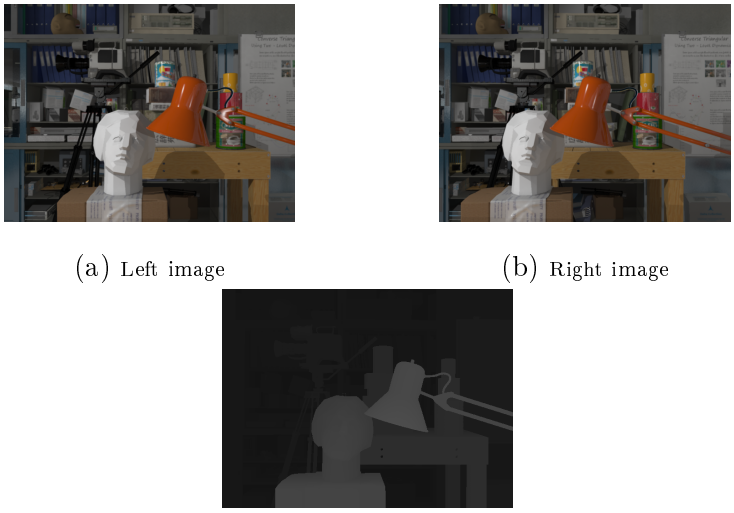

(a) Left image

(b) Right image

(c) Disparity map

Figure 1.10: Stereo pair and disparity map

In general, stereo matching algorithms can be categorized into two major classes:

- local methods
- global methods.

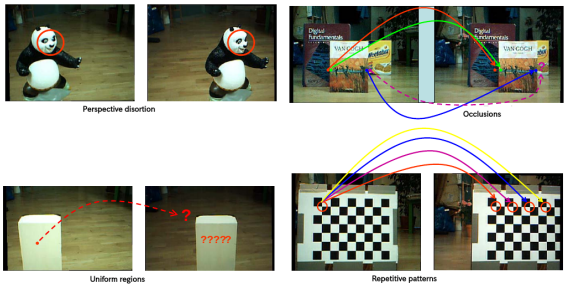

Figure 1.11: Stereo matching general problems

Local stereo algorithms estimate the correspondence using a local support region or a window. Local algorithms generally rely on an approximation of the smoothness constraint assuming that all pixels within the matching region have the same disparity. However, this assumption is not valid for highly curved surfaces or around disparity discontinuities.

A naive approach consists of comparing each pixel or window in the left image with every pixel or window on the same epipolar line in right image and picking position with minimum match cost (e.g., SSD, SAD, normalized correlation).

Global stereo methods consider stereo matching as a labeling problem where

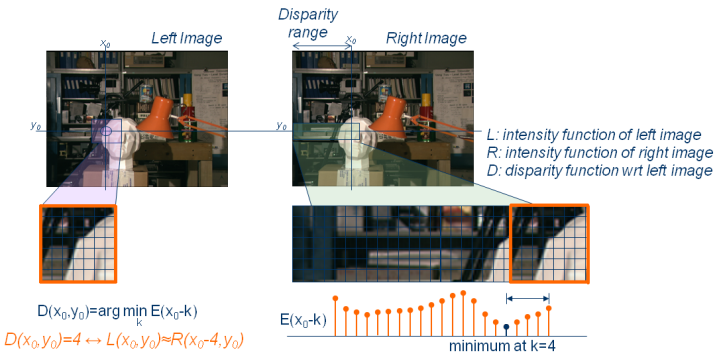

Figure 1.12: Local stereo matching, window based

the pixels of the reference image are nodes and the estimated disparities

are labels. An energy functional embeds the matching assumptions by its data, smoothness, and occlusion terms and propagates them along the scan line or through the whole image. The labeling problem is solved by energy functional minimization, using dynamic programming, graph cuts, or belief propagation.
Even if this class of algorithms is significantly slow, the results, especially when textures and discontinuities are present, are much accurate.

In this thesis the Kolmogorov and Zabih's Graph Cuts Stereo Matching Algorithm, [1], has been used, because there were no time constraints requirements and the quality of the computed disparities has been considered satisfying with regard to the ground trouth.

(a) Left image

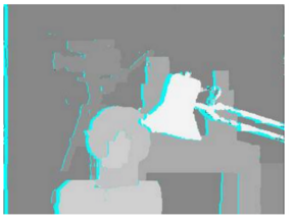

(b) Graph cuts' disparity map

(c) Ground truth disparity map

Figure 1.13: Results of the Kolmogorov and Zabih's graph cuts algorithm on the Tsukuba pair

In this algorithm the correspondence problem is addressed by constructing a problem representation and an energy function that takes into account the *uniqueness* of a configuration.

A configuration f is any map $f : \mathcal{A} \to \{0, 1\}$, where $\mathcal{A}$ is the set of pair of pixels (p, q), (p pixel of left image and q pixel of right image), which may potentially correspond. If $a = (p, q)$ is an assigment, then $f(a) = 1$ means that p and q correspond under the configuration f.

A configuration is *unique* if for all pixels p (resp. q), there is at most one active assignment involving p (resp. q): for instance, considering p, if $f(p, q1) = f(p, q2) = 1$, then $q1 = q2$. A pixel that correspond to no pixel in the other image is labeled as occluded.

The energy of a configuration f is defined as:

$$E(f) = E_{data}(f) + E_{occlusion}(f) + E_{smoothness}(f) + E_{uniqueness}(f) \qquad (1.1)$$

where each term promotes a desired property of the configuration: the data term measures how well matched pairs fit, the occlusion term minimizes the number of occluded pixels, the smoothness term penalizes the nonregularity of the configuration, and the last term enforces the uniqueness.

Since this energy funtion is not graph-representable, his minimization can be approximated by an iterated constrained minimization, given by so-called expansion moves []; given this changes, the energy assumes a new expression, $E_{f,\alpha}$.

The minimal cut of a graph that represents the energy $E_{f,\alpha}$ is then found. The problem is NP-hard, so a local minimum is computed.

1.2 3D capturing devices

For stereoscopic shooting, two synchronized cameras must be used. The distance between the center of the lenses of the two cameras is called the interaxial, and the cameras' convergence, is called the angulation. These two parameters can be modified according to the expected content peculiarities.

The two cameras must be correctly aligned, identically calibrated (i.e.

Figure 1.14: Interaxial separation between lenses

brightness, color, etc...) and perfectly synchronized (frame-rate and scan-wise).

To hold and align the cameras, a stereo-rig is used; the rigs can be of two main types:

- the side-by-side rig, where the cameras are placed side by side (Figure 1.15a). This kind of 3D-rig is mostly useful for large landscape shots since it allows large interaxials; however, it doesn't allow small interaxials because of the physical size of the cameras;

- the beamsplitter rig (Figure 1.15b), where one camera films through a semi-transparent mirror, and the other films the reflection in the mirror. These rigs allow small and medium interaxials, useful for most shots, but not the very large interaxials (because the equipment would

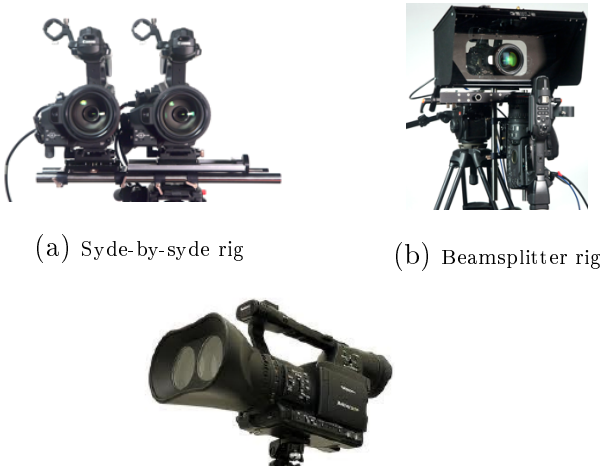

(a) Syde-by-syde rig

(b) Beamsplitter rig

(c) Monoblock camera

Figure 1.15: Professional technologies for 3D TV

be too large and heavy).

Monoblock cameras have been designed as well, where the two cameras are presented in a fixed block and are perfectly aligned, which avoids cameras desynchronization (Figure 1.15c).

A second category of 3D shooting devices is presented in Figure 1.16. These electronic devices are less expensive and are targeting the user-created stereoscopic picture/movie distribution.

An other important category of 3D image capture devices it's the one employed in the robotics and automation field. They are usually impressively precise, cost-efficient and fast.

1.3 3D video displays

The basic technique of stereo displays is to present offset images that are displayed separately to the left and right eye. Both of these 2D offset images

(a) Mobile phones

(b) Digital cameras

(c) Camcorders

Figure 1.16: Digital personal stereo vision systems

(a) The Bumblebee series from Point Grey

(b) Human wearable stereo device

Figure 1.17: Industrial and robotic stereo cameras

are then combined in the brain to give the perception of 3D depth.

For stereoscopic 3D displays the viewer needs to wear special glasses which separate the views of the stereoscopic image for the left and the right eye. These 3D glasses can be active or passive.

On the one hand, active glasses are controlled by a timing signal that allows to alternatively darken one eye glass, and then the other, in synchronization with the refresh rate of the screen. Hence presenting the image intended for the left eye while blocking the right eye's view, then presenting the right-eye image while blocking the left eye, and repeating the process at a high speed

which gives the perception of a single 3D image. This technology generally uses liquid crystal shutter glasses(Figure 1.18a).

On the other hand, passive glasses are polarization-based systems and contain a pair of opposite polarizing filters; each of them passes light with similar polarization and blocks the opposite polarized light (Figure 1.18b). Passive 3D TV screens sport a filter with alternating horizontal and vertical stripes, separated by a black, picture-blanking bars. When used with glasses which have corresponding polarising lenses, alternate frames are presented to each eye to create a 3D image.

The color anaglyph-based systems are a particular case of the passive glasses and use a color filter for each eye, typically red and cyan, Figure 1.18c . The anaglyph 3D image contains two images encoded using the same color filter, thus ensuring that each image reaches only one eye.

(a) LCD shutter glasses

(b) Polarized glasses

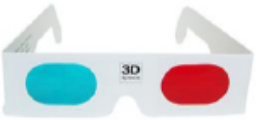

(c) Anaglyph glasses

Figure 1.18: Passive and active glasses for 3D viewer technologies

Chapter 2

Stereo video watermarking

2.1 Watermaking

Digital watermarking consists in imperceptiby and persistently associating some extra information with some original content.
The basic watermarking workflow is presented in Figure 2.1.

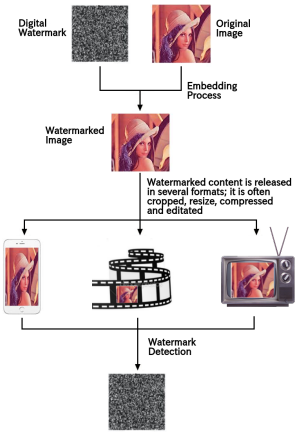

Figure 2.1: Watermarking workflow

2.1.1 Properties

Three parameters are required to evaluate watermarking technique performances:

- transparency, that is the misure of how much the watermark affects the quality of the host data;
- robustness, i.e.,the capability of the hidden data to survive host signal manipulation including compression, signal processing, geometric manipulations;
- data payload, that is the amount of data of information bits that it is able to convey.

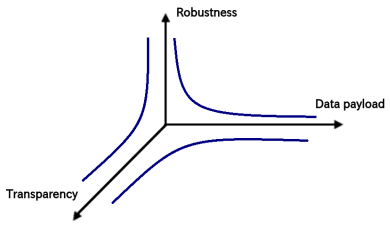

Figure 2.2: Watermark properties trade-off

Finally, a watermarking technique can be:

- non-blind/blind, if at the decoder side the original content is available or not, respectively;
- private/public if only authorized users can recover it or if anyone to read the watermark, respectively;
- detectable/readable, if it is only possible to decide whether a given watermark is embedded in the content or if the bits hidden in the content can be read without knowing them in advance, respectively.

2.1.2 Embedding domains

Host features modified during embedding can belong to

- spatial domain: the watermark is embedded by directly modifying the pixel values;

Figure 2.3: Spatial domain watermark insertion

- frequency domain: the image is transformed through a mathematical transformation, some coefficients are modified and finally the inverse transform is carried out;

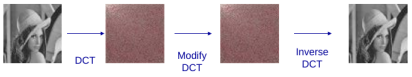

Figure 2.4: Frequency domain watermark insertion

- hybrid techniques: a block wise transform is applied, the image is divided into blocks and for each block a mathematical transformation is computed, some coefficients are modified and the inverse transform is done.

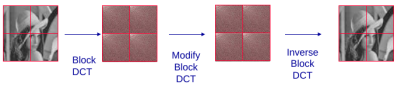

Figure 2.5: Hybrid technique

2.1.3 Embedding techniques

The most straightforward ways to add a watermark in a given content have been proved to be Spread Spectrum (SS) approach and Side Information (SI). As in spread spectrum communications, the former approach considers the

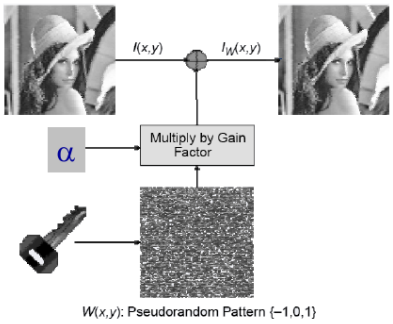

Figure 2.6: Spread spectrum technique

original content as a signal and the watermark as a noise that is spread over very many frequency bins so that the energy in any one bin is very small and certainly undetectable.
The latter takes advantage of the fact that the original content is known at the embedder side (but unknown at the detector): this way the watermark can be modulated according to the original and the quantity of inserted data can be maximed.

Sometimes hybrid watermarking methods combining spread spectrum and side information concepts can be applied; they try to benefit from both the robustness and transparency of the spread spectrum methods and the increased data payload of the side information methods.

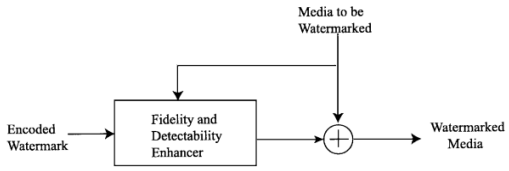

Figure 2.7: Side information technique scheme

2.2 Stereoscopic video watermarking

In the literature, stereoscopic video watermarking has been initially approached as a direct extension of still image watermarking, i.e. by considering the right and the left views as two independent images. This way, the stereo data can be straightforward exploited with basic 2D methods. However, such straightforward application does not consider the peculiarities of the stereoscopic video content, therefore a second modality considers derived representations from the stereo pair, as a disparity map.
A new approach, however, has been recently introduced in stereoscopic view-based methods: disparity-coherent watermarking [3].

2.2.1 Embedding domain

In stereoscopic video context the studies can be structured in two other categories in addition to spacial and frequency domain:

- view-based methods;

- disparity-based methods

according to the reference image in which the mark is actually inserted.
In Figure 2.8 the workflows of both methods are presented.

The predilection direction in the literature is represented by the view-based watermarking approaches, which are currently deployed for stereo-

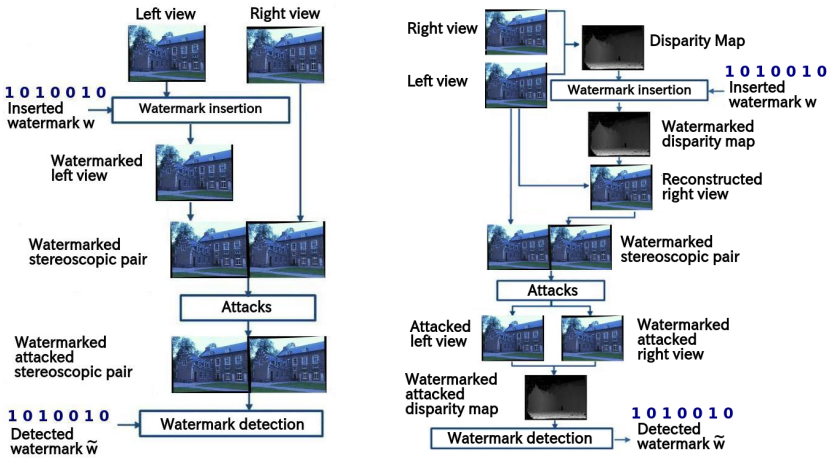

(a) View-based watermarking workflow

(b) Disparity-based watermarking workflow

Figure 2.8: Stereoscopic video watermarking workflow

scopic still images.

In this context disparity-coherent watermarking has been introduced, [3], to provide superior robustness against virtual view synthesis, as well as to improve perceived fidelity.

Disparity-coherence refers to the fact that a physical point of the captured scene should carry the same watermark sample regardless of where it appears in the left/right view.

The advantages of producing disparity-coherent watermarks are two: first it produces pairs of stereoscopic views that are more in line with what would naturally occur in reality and thereby yields less visual discomfort, second disparity-coherent watermarks are expected to exhibit superior robustness against view synthesis, [3].

View synthesis consists in generating a virtual view in-between views that are available, e.g.the left and right views in stereo video.

2.2.2 Transparency evaluation

The visual quality of the watermarked content in images and 2D video is usually objectively evaluated by five objective measures, namely, the PSNR, IF, NCC, SC, and SSIM .

In this thesis the measures in [2] have been used to evaluate the quality of the watermarking technique in terms of transparency.
In Chaminda et al.'s study a Reduced-Reference (RR) quality metric for color plus depth 3D video compression and transmission is proposed, using the extracted edge information of color plus depth map 3D video.
The work is motivated by the fact that the edges/contours of the depth map can represent different depth levels and this can be considered for measuring structural degradations. Since depth map boundaries are also coincident with the corresponding color image object boundaries, edge information of the color image and of the depth map is compared to obtain a quality index (structural degradation) for the corresponding color image sequence.
In order to quantify structural comparison, luminance comparison and contrast comparison parameters for the depth map and corresponding watermarked views, a modified version of the commonly used SSIM metric is adopted:

$$Q_{Depth}(x,y) = [l(x,y)]^{\alpha} \cdot [c(x,y)]^{\beta} \cdot [S_{Depth}(x',y')]^{\gamma} \tag{2.1}$$

where $l(x,y)$ and $c(x,y)$ are luminance and contrast comparisons performed on original depth maps and the ones computed after watermarking, respectively, and $S_{Depth}(x',y')$ is the structural comparison between the gradient/edge maps of original and post-watermarking computed depth map images.

Then the overall depth map quality is calculated as

$$MQ_{Depth}(X,Y) = \frac{1}{M}\sum_{j=1}^{M} Q_{Depth}(x_j, y_j). \tag{2.2}$$

The SSIM-based quality index for the color image can be described as follows:

$$Q_{View}(x,y) = [l(x,y)]^{\alpha} \cdot [c(x,y)]^{\beta} \cdot [S_{View}(x',y')]^{\gamma} \tag{2.3}$$

where $l(x,y)$ and $c(x,y)$ are luminance and contrast comparisons performed on original and watermarked views, respectively, and $S_{View}(x',y')$ is the structural comparison between the gradient/edge maps of the gradient maps of the corresponding original depth map and the watermarked views.
Hence, the overall color image quality is calculated as

$$MQ_{View}(X,Y) = \frac{1}{M}\sum_{j=1}^{M} Q_{View}(x_j, y_j). \tag{2.4}$$

As in [2], the Sobel operator has been selected to obtain edge information (i.e., the binary edge mask) due to its simplicity and efficiency.

2.2.3 Robustness

View synthesis

Since in stereoscopic video context it is rather common practice to generate intermediate virtual views to adjust depth perception and since such view synthesis introduces non-rigid local geometric distortion that are not properly tackled by state-of-the art resynchronization mechanisms, stereo video watermarking strategies have to achieve robustness to synthetic view synthesis.

In this thesis a disparity-coherent watermarking algorithm has been implemented. It works in the frequency and spatial domain: a pseudo-random sequence of real numbers is embedded in a selected set of DFT coefficients of the left image then the reference watermark is spatially inserted in a disparity-coherent way in the right view.
It has shown good results in quality measure tests and roubustness test against view synthesis.
An optimum criterion to verify if a given mark is present in an image is derived based on statistical decision theory, [4], allowing a robust watermark detection without resorting to the original uncorrupted image.

Chapter 3

Spatial disparity-coherent watermarking

As said in the previous chapter, a number of works focused on how to incorporate depth information into the perceptual shaping process of the embedded watermark.
This process allows to achive disparity-coherence and makes sure that a physical point of the captured scene carries the same watermark sample regardless of where it appears in the left and right view.

This process brings two advantages: it produces stereoscopic views more in line with reality, therefore yields less visual discomfort; and it is expected to have superior robustness against view synthesis.

3.1 Prior work

A prior work that is based on the disparity-coherent technique is the one carried on by Doerr et al in "Blind Detection for Disparity-Coherent Stereo Video Watermarking" [].

The watermark strategy assumes that the key-seeded reference watermark pattern $w_K \tilde{} N(0,1)$ is embedded spatially in the left view and subsequently transferred to the right one.

The watermark embedding and detection operations for the left view are therefore given by the conventional spread-spectrum equations:

$$f_l^w = f_l + \alpha w_K$$

$$\rho(f_l + \epsilon\alpha w_K, w_K) = \frac{1}{wh}\sum_{x,y}(f_l(x,y) + \epsilon\alpha w_K(x,y))w_K(x,y) \approx \epsilon\alpha$$

where the superscript w indicates watermarked quantities, the subscript l (resp. r) denotes quantities related to the left (resp. right) view, $\alpha > 0$ is the embedding strength, and w is normally distributed with zero mean and unit variance.

The embedding strenght used in [] to keep the embedding distortion imperceptible is $\alpha = 3$.

For the right view, the watermarking equation is the same, except that the watermark pattern w_K is warped according to the depth information prior to insertion.

$$\forall(x,y) \in [1:w][1:h] f_r^w(x,y) = f_r(x,y) + \alpha w_K(x + d(x,y), y) = f_r + \alpha w_K^d(x,y)$$

The watermark detection on the right view relies on the computation of a horizontal cross-correlation array.

$$\rho(f_r + \epsilon\alpha w_K^d, w_K^s) \approx \epsilon\alpha D_s$$

$$\rho = \epsilon\alpha[D_{smin}, .., D_0, .., S_{smax}]$$

where D_s is the proportion of pixels whose disparity value is exactly equal to s.

The correlation array is then mapped into a scalar value in order to compare it with a threshold and to decide whether the tested content contains the watermark. Authors proposed three possible mapping functions:

$$\rho_{max} = \max_s \rho[s]$$

$$\sum_s \rho[s]$$

$$\sum_{|rho[s]|>\tau_\rho} |\rho[s]|$$

3.2 Gaussian-noise disparity-coherent watermarking

Based on the described technique, we propose a new spatial watermarking technique.

For the spatial watermark its been taken under consideration the insertion of a Gaussian-noise reference watermark in an additive way.

As in Doerr et al, the left view is processed in the conventional way, with spred-spectrum equations (riferimento all'equazione); the watermark is then warped according to the disparity value and inserted in the right view (rif all'eq), taking under consideration that the occluded zones shoudn't be processed.

The added pattern and the reference images have the same size, so it should be noted that the warping process will generate a loss of marked pixel, due to the baseline's lenght.

Since the disparity map and the occclusion map are usually not available,

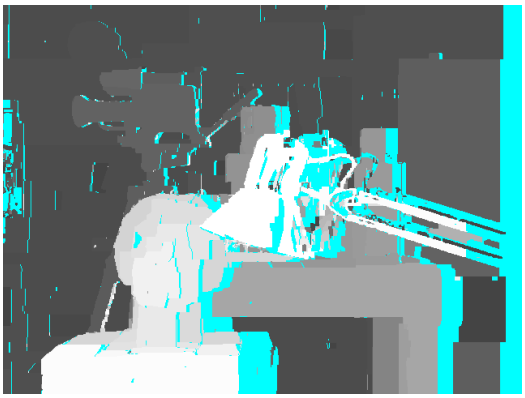

Figure 3.1: disparity left-to-right computed with KZ

it needs to be estimated through the KZ algorithm, before the warping process.

The embedding strenght is $\alpha = 1$; it should be noted that this baseline watermarking framework could be enriched with conventional add-ons, e.g. perceptually modulate the embedding strength to better accommodate for the human visual system or canceling host interference for improved detection statistics.

In the detection process, it has been used a conventional correlation-based detector for the left view (ref to eq).

On the other hand to detect the watermark in the right view two differet correlation-based strategies are proposed: in the first strategy we computed the correlation value between the non-distorted watermark and the right view warped according to the right-to-left disparity, this way the priviously

warped watermark is restored, even if there will be discontinuities due the occluded zones. In formula:

$$\rho((f_r + \epsilon\alpha w_K^*)^*, w_K) = \frac{1}{wh}\sum_{x,y}(f_r(x,y) + \epsilon\alpha w_K^*(x,y))^* w_K(x,y) \approx \epsilon\alpha$$

where the superscript * indicates the warped mark/image.

The second strategy is again a simple correlation-based detector, but the correlation value is computed between the right view and the warped watermark instead of the original one, based on the fact that the right view should contain this, rather than the reference pattern and that the reciever can compute the disparity map thats needed to warp the mark and perform the detection.

$$\rho(f_r + \epsilon\alpha w_K^*, w_K^*) = \frac{1}{wh}\sum_{x,y}(f_r(x,y) + \epsilon\alpha w_K^*(x,y)) w_K^*(x,y) \approx \epsilon\alpha$$

To illustrates the performance of the binary classifier system as its discrimination threshold is varied it has been drawn the corresponding ROC curve.
The ROC curve is a representation of the sensitivity as a function of fall-out. The curve is created by plotting the true positive rate (TPR) against the false positive rate (FPR) at various threshold settings.
The true-positive rate is also known as sensitivity and the false-positive rate is also known as the fall-out.

As said before the disparity-coherent watermarking have the ability to detect the embedded watermark in synthetized views: to performe the detection on a random right view, that might be synthetized, the detector will

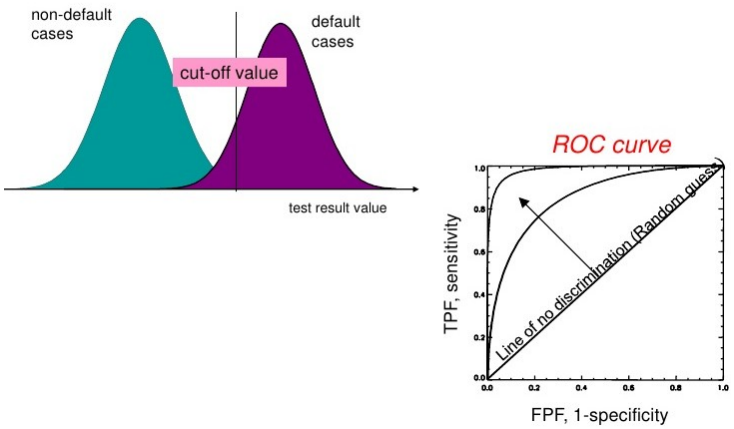

Figure 3.2: ROC curve explanation

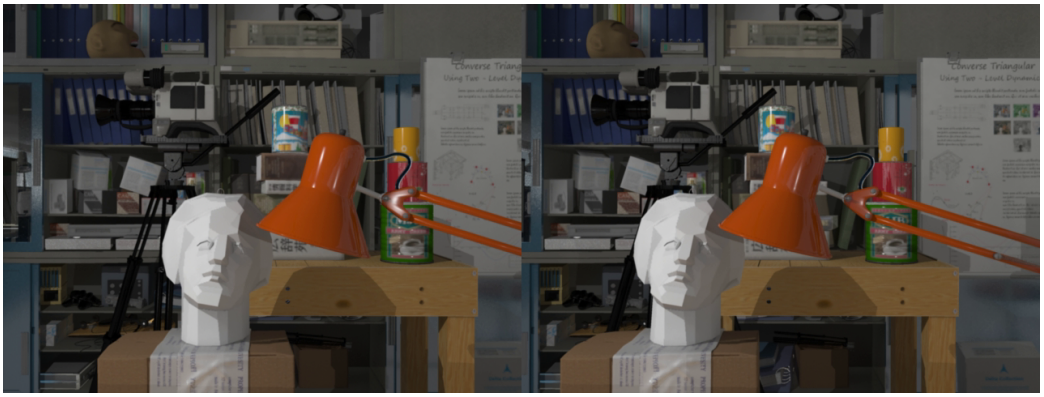

Figure 3.3: stereo image marked with spatial algorithm with power equal to 1

need to calculate the disparity map between the analyzed view and the recieved left, and warp it accordingly, to recompose the original watermark. There is then a tight bond between the watermarking process and the evaluation of the disparity maps; with the graph-cuts algorithm it's possible to compute accurate maps and to know the occluded zones.

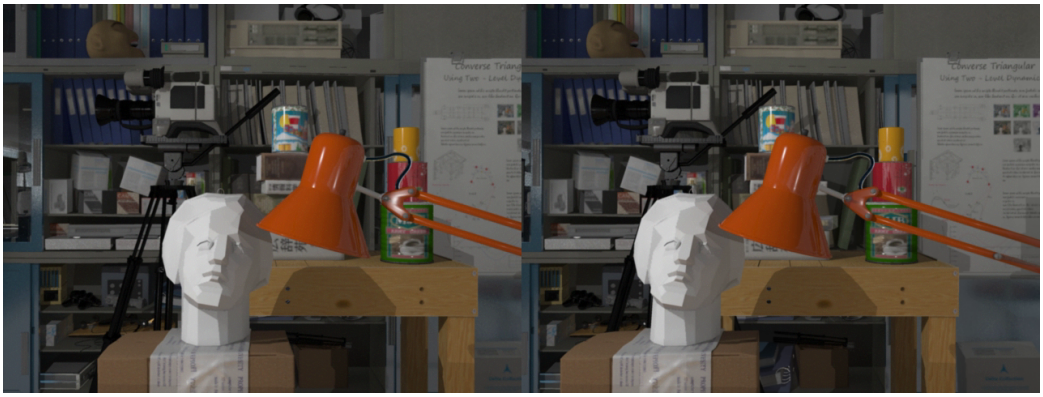

Figure 3.4: stereo image marked with spatial algorithm with power equal to 1

Chapter 4

Frequency disparity-coherent watermarking

Now we proposed a variant of the described watermarking process, which works in the frequency domain.

4.1 Watermark in Fourier domain

The strategy is based on the technique presented by Piva et al in "Improving DFT Watermarking robustness through optimum detection and synchronisation" [], where a watermarking algorithm for digital images operating in the frequency domain is presented: the method embeds a pseudo-random sequence of real numbers in a selected set of DFT coefficients of the image. Moreover, a synchronisation pattern is embedded into the watermarked image, to cope with geometrical attacks, like resizing and rotation. After embedding, the watermark is adapted to the image by exploiting the masking characteristics of the Human Visual System, thus ensuring the watermark invisibility.

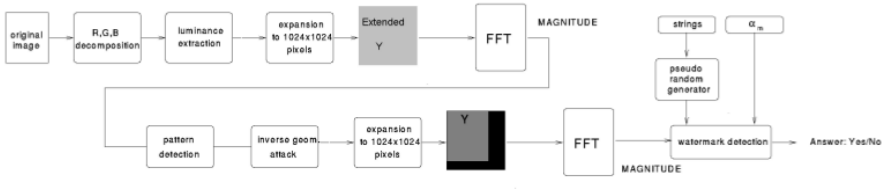

Figure 4.1: watermarking algorithm

For the stereo watermarking task this process has been simplified and cut to the basic frequency watermaking.

4.1.1 Watermark embedding

In [] the watermark is embedded in a subset of DFT coefficients of the luminance Y.

Since a traslation of the scene will only change the phase values of the DFT, leaving unaltered the magnitude values, the watermak only concernes the latter, to achieve robustness against image traslation.

To garantee a blind detection system the number and position of the coefficient are fixed a priori: based on the size of the image to watermark, the coefficient are choosen in the medium frequencies of the spectrum to achieve a compromise between robustness and invisibillity.

The watermark embedding rule is the following:

$$y_i^{'} = y_i + \alpha m_i y_i$$

where $y_i^{'}$ represents the watermarked DFT magnitude coefficient, y_i the corresponding original, m_i is a sample of the watermark sequence, and α is the watermark energy.

The inverted DFT is then applied to obtain the watermarked luminance $Y^{'}$.

4.1.2 Watermark detection

To determine if a given image luminance Y either embedds or not the reference watermark in [] a threshold-based detection is used.
The luminance of the received image is extracted and its DFT trasform is computed; from the obtained magnitude matrix the right coefficents can be selected since their positions are known as said above.
Knowing the seed (in the shape of two strings, one numeric one alphanumeric) the watermark can be reproduced.

To verify if the selected coefficients have been altered by means of the watermark it is used a statistical decision theory: two hypotheses are defined, the image contains the reference watermark (hypotheses H_1) or the image does not contain this mark (hypotheses H_0). Relying on Bayes theory of hypothesis testing, the optimum criterion to test H1 versus H0 is minimum Bayes risk; the test function results to be the likelihood ratio function L that has to be compared to a threshold:

- if $L > \lambda$, the watermark m^* is present;
- if $L < \lambda$, the watermark m^* is absent.

To choose a proper threshold, it has been chosen to fix a constraint on the maximum false positive probability and the optimum decoder is designed refferring to the Neyman-Pearson criterion, as:

$$L(y) = \sum_{i=0}^{N-1}[-\beta ln(1+\alpha_m m_i^*)] + \sum_{i=0}^{N-1}[-(\frac{y_i}{\alpha_i(1+\alpha_m m_i^*)})^{\beta_i} + (\frac{y_i}{\alpha_i})^{\beta_i}]$$

and

$$\lambda = 3.3\sqrt{2\sum_{i=0}^{N-1}[\frac{[(1+\alpha_m m_i^*)^{\beta_i}]}{(1+\alpha_m m_i^*)^{\beta_i}}]+\sum_{i=0}^{N-1}\{\frac{[(1+\alpha_m m_i^*)^{\beta_i}-1]}{(1+\alpha_m m_i^*)^{\beta_i}}\}-\sum_{i=0}^{N-1}[\beta_i ln(1+\alpha_m m_i^*)]}$$

In () $m^* = \{m_i^*\} i = 0, 1, ...N-1$ is the watermark, α_m the mean watermark energy, α_i and β_i are statistic parameters describing the probability density function shape of the magnitude of the watermarked DFT coefficients y_i.

The values of this parameters are choosen by means of Maximum Likelihood criterion, based on the the fact that the coefficients belonging to small subregions of the spectrum are characterised by the same statistic parameters and follows a Weibull distribution, modeled as:

$$f(y_i) = \frac{\beta}{\alpha}(\frac{y_i}{\alpha})^{\beta-1}\exp\{-(\frac{y_i}{\alpha})^{\beta}\}$$

In summary, the detection process can be decomposed in the following steps:

- generation of the watermark m^*;
- estimation of the parameters α, β into the regions composing the watermarked area of the spectrum;
- computation of $L(y)$ and λ ;
- comparison between $L(y)$ and λ ;
- decision.

The decoder can detect the watermark presence also in highly degraded images. In particular, the system is robust to sequences of different attacks, such as rotation, resizing, and JPEG compression, or such as cropping, resizing and median filtering.

4.2 Stereo watermarking embedding

For the stero-marking process its been taken under consideration a 512x512 subset of pixel of the image, in particular we focused in marking the part of the scene which is common to both the left and right view.

Figure 4.2: cropped image to watermark

The left view is then processed with the algorithm discribed above.

To watermark the right view the pattern is created ad-hoc: a signal of the watermak is generated using the phase of the left image and the phase of the reference watermark and the coefficients of the right view.
This way the right view will be marked with its coefficient, but with the correct phase, and the corresponding pixel in the left and right view will present the same alteration, not to cause visual distorsions.

$$l_w = l + \frac{1}{MN}\sum\sum(\alpha|L(u,v)||w|\exp\{j(\phi_l+\phi_w)\})\exp\{+j2\pi(\frac{ux}{M}\frac{vy}{N})\}$$
$$r_w = r + \frac{1}{MN}\sum\sum(\alpha|R(u,v)||w|\exp\{j(\phi_l+\phi_w)\})^*\exp\{+j2\pi(\frac{ux}{M}\frac{vy}{N})\}$$

The watermark is then brought back in the spatial domain with the inverse Fourier trasform, the image is warped according to the left-to-right disparity and added spatially to the right view.

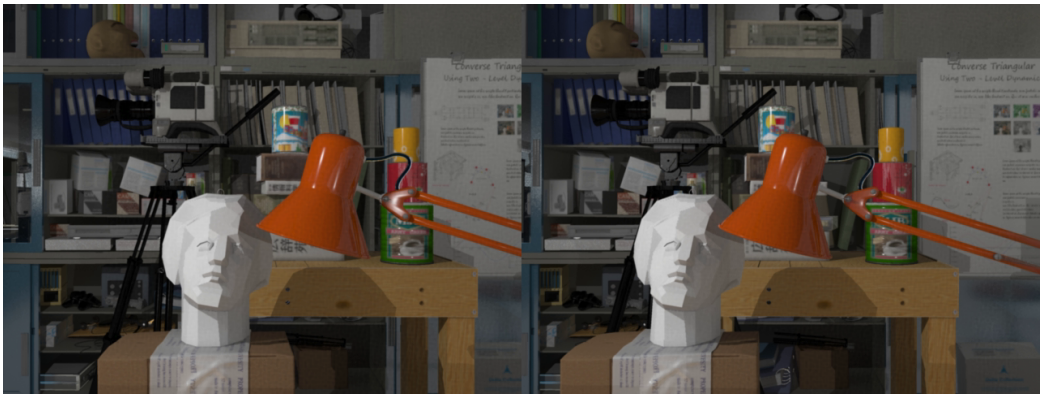

Figure 4.3: stereo image marked with DFT algorithm with power equal to 0.3

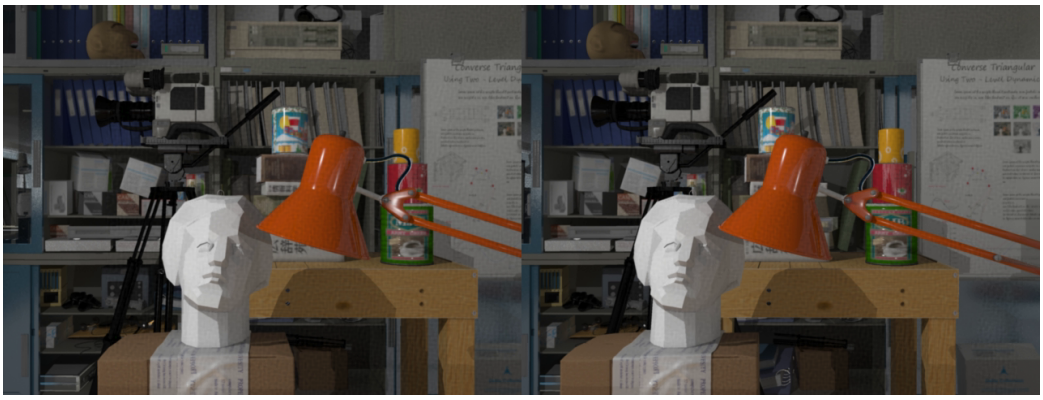

Figure 4.4: stereo image marked with DFT algorithm with power equal to 0.5

4.3 Stereo detection algorithm

The detection of the watermark is performed with the detector implemented by Piva et al.

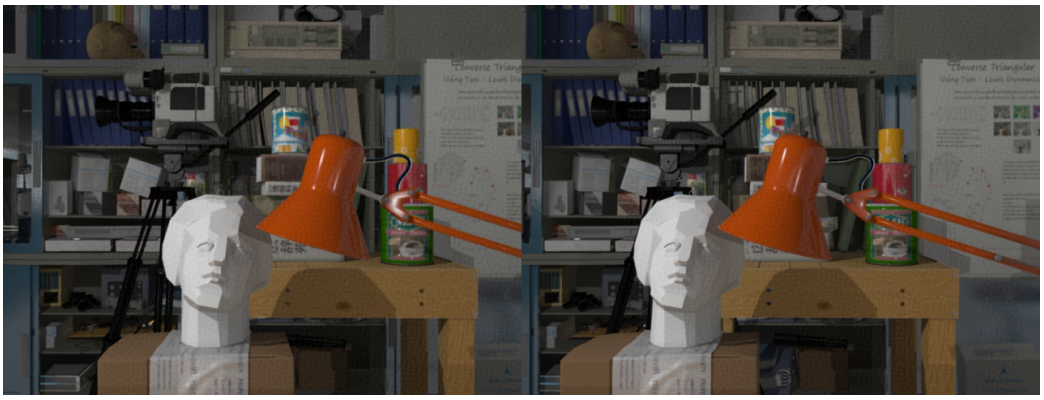

Figure 4.5: stereo image marked with DFT algorithm with power equal to 0.6

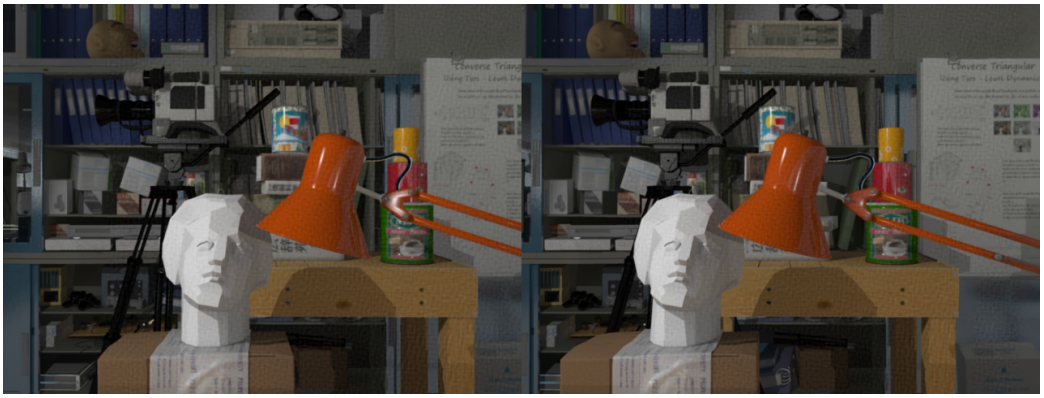

Figure 4.6: stereo image marked with DFT algorithm with power equal to 0.7

As for the embedding process, the algorithm is applied to the left view without changes, meanwhile, some adaptations are needed for the right view detection.

First the detection algorithm computes the right-to-left disparity, then the right view is warped accordingly to ricreate the phase of the inserted watermark; to mantain the correctt phase the occluded zones are filled with the pixels of the recieved left view (taking under consideration that this little amount of image's pixel would not influence the detection).

The created image is then processed by the threshold-based detection algorithm.

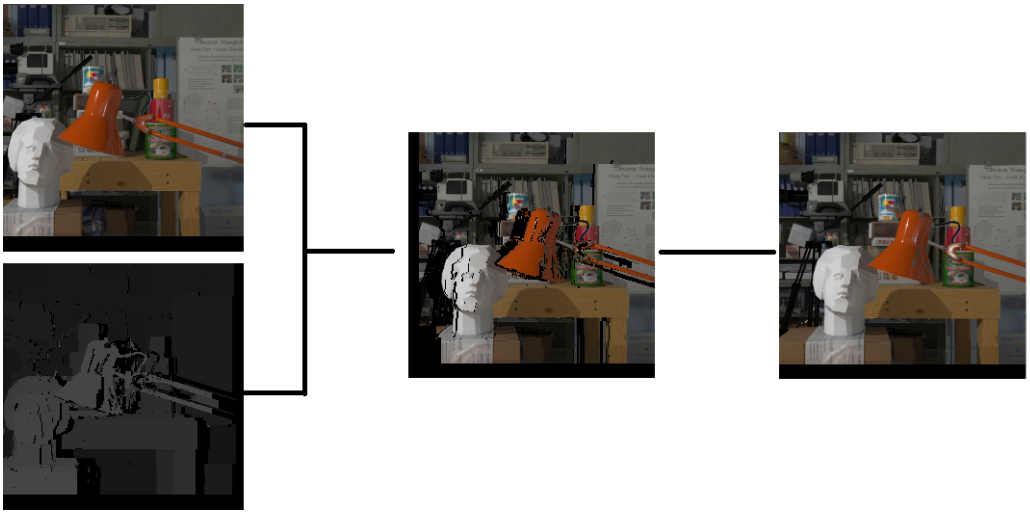

Figure 4.7: detection workflow

Chapter 5

Experimental Results

The proposed method has been tested to verify its validity in terms of robustness and transpaency.
As said before, robustness is the ability of the watermark to cope with the degradation of the image due to compression, view synthesis etc.
Another important feature of a good watermarking method is transparency, such that human eye could not distinguish the dissimilarities between the watermarked image and the original one.
In this chapter will be presented the results carried out to test the algorithm performances.

The marking process its been applied to a 1 minute stereo-video sequence created starting from the left and right view of the new Tzukuba dataset, with GOP of 60 frames and 30 fps.
Its been chosen to mark every 60 frames, i.e. only the I frame of each GOP.
The frames of the reference video has been marked with different power and new marked videos has been created with different levels of compression.

The compressed videos are made with the `ffmpeg` library, changing the Constant Rate Factor (CRF), the default quality setting for the x264 encoder. The value can be set in a range between 0 and 51, where lower values would result in better quality (at the expense of higher file sizes).

5.1 Robustness against compression

In video analysis, compression is useful because it helps reduce resource usage, such as data storage space or transmission capacity.
This process brings to a degradation of the image due to the compression ratio, thus a degradation of the watermark.
To prevent this problem a solution can be to improve the strenght of the embedded watermark, but its necessary to mantain an acceptable trade-of between robustness and transparency.

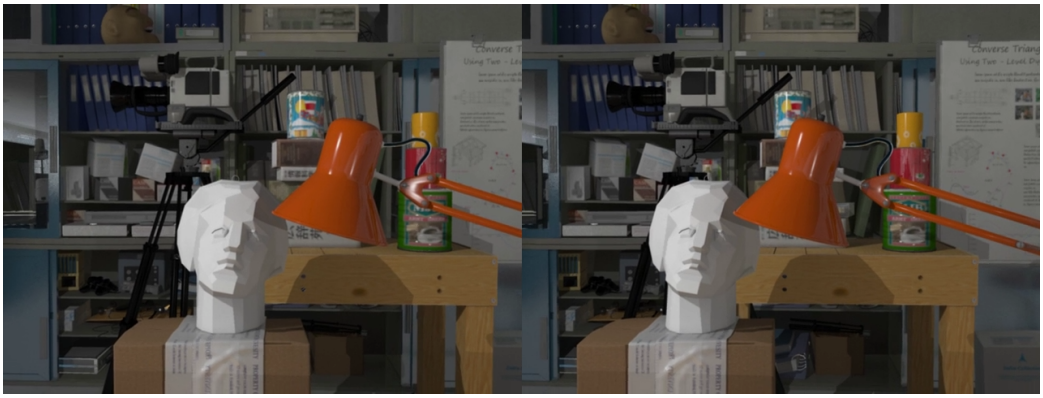

Figure 5.1: stereo image from video marked with power 0.3 and compressed with crf equal to 1

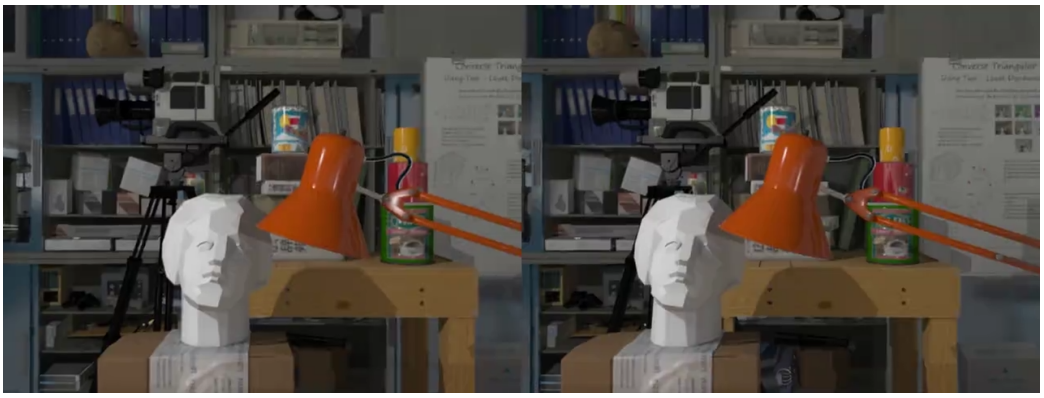

Figure 5.2: stereo image from video marked with power 0.3 and compressed with crf equal to 30

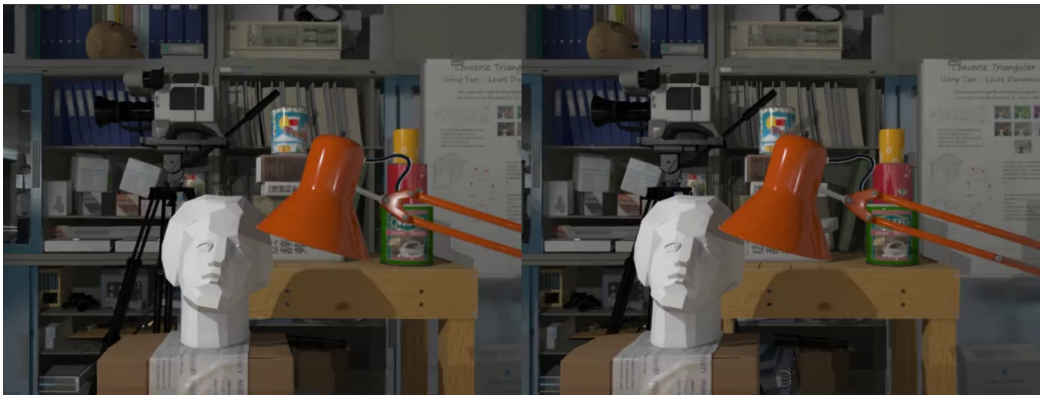

Figure 5.3: stereo image from video marked with power 0.3 and compressed with crf equal to 25

5.1.1 Robusteness in spatial watermarking

In spatial domain watermarking systems, the watermark is embedded directly in the spatial domain (pixel domain).
Many of the spatial watermarking techniques provide simple and effective schemes for embedding an invisible watermark into an image, but are less robust to common attacks such as lossy compression.

The evaluation of this detection system has been studied through the

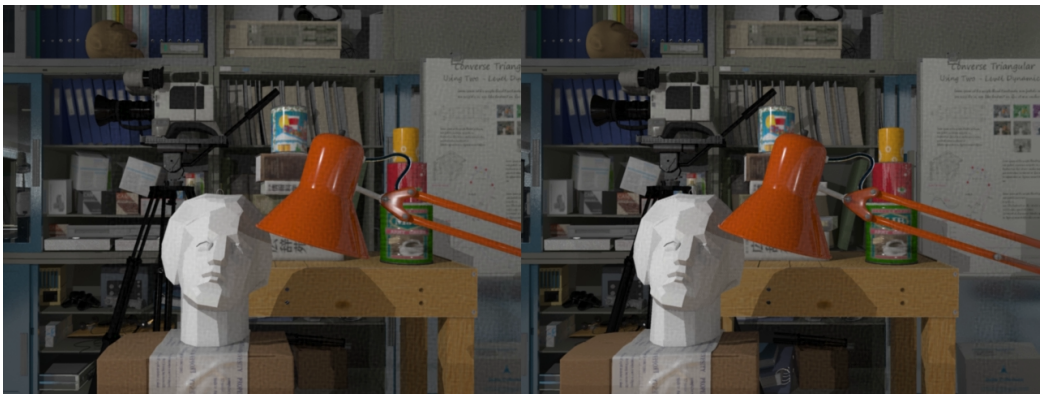

Figure 5.4: stereo image from video marked with power 0.6 and compressed with crf equal to 1

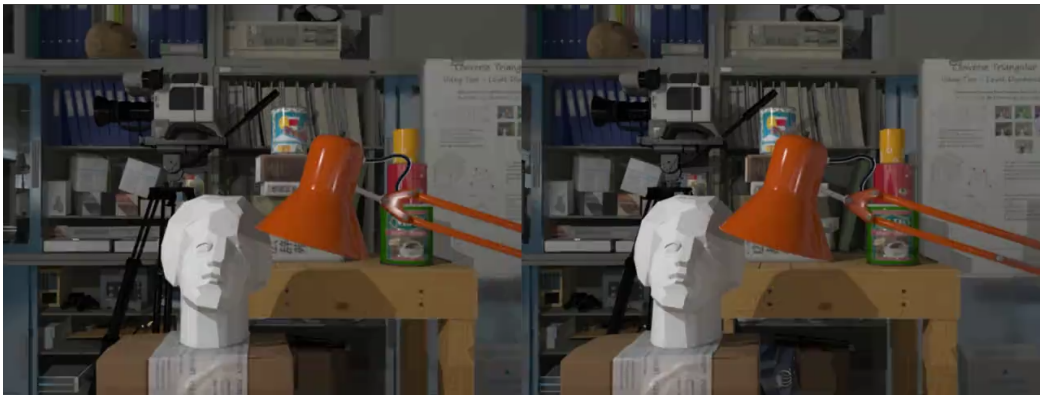

Figure 5.5: stereo image from video marked with power 0.6 and compressed with crf equal to 30

ROC curve has said in chapter 3. The results are shown below.

5.1.2 Robustess in DFT watermaking

In transform domain watermarking systems, watermark insertion is done by transforming the image into the frequency domain using a discrete Fourier transform (DFT), full-image DCT, block-wise DCT, wavelet, Hadamard, Fourier-Mellin, or other transforms.

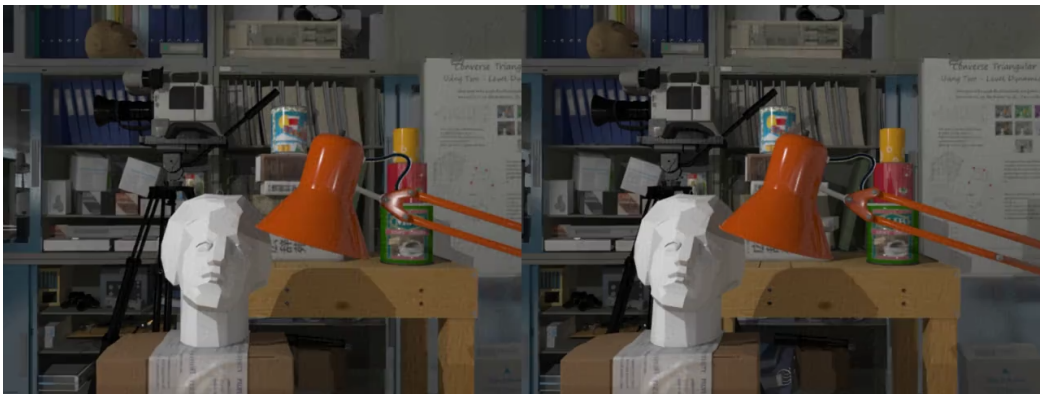

Figure 5.6: stereo image from video marked with power 0.6 and compressed with crf equal to 25

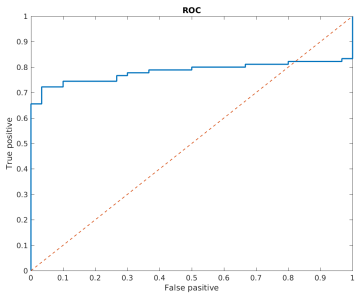

Figure 5.7: ROC curve of a spatial marked image with power equal to 1 and not compressed

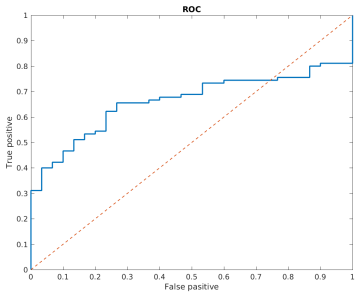

Figure 5.8: ROC curve of a spatial marked image with power equal to 1 and compressed with crf 15

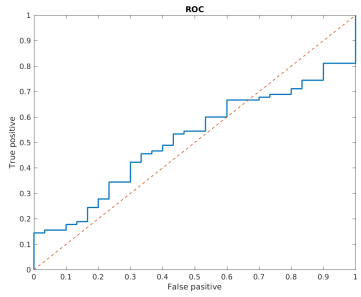

Figure 5.9: ROC curve of a spatial marked image with power equal to 1 and compressed with crf 25

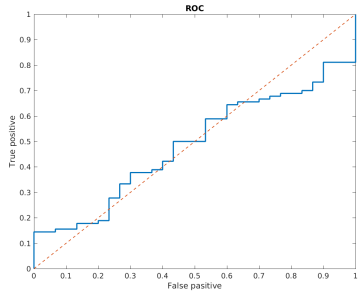

Figure 5.10: ROC curve of a spatial marked image with power equal to 1 and compressed with crf 30

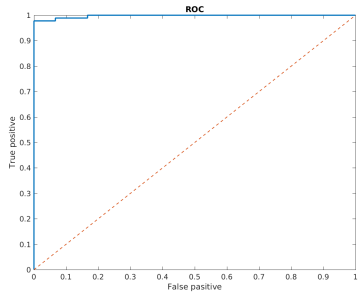

Figure 5.11: ROC curve of a spatial marked image with power equal to 3 and not compressed

It is often claimed that embedding in the transform domain is advantageous in terms of visibility and security.

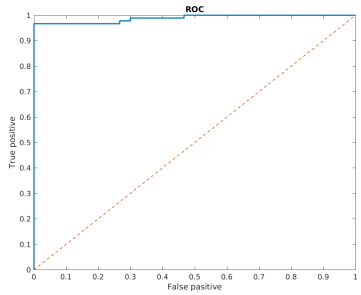

Figure 5.12: ROC curve of a spatial marked image with power equal to 3 and compressed with crf 15

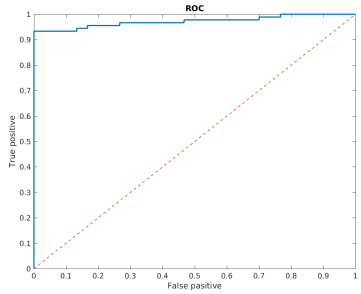

Figure 5.13: ROC curve of a spatial marked image with power equal to 3 and compressed with crf 25

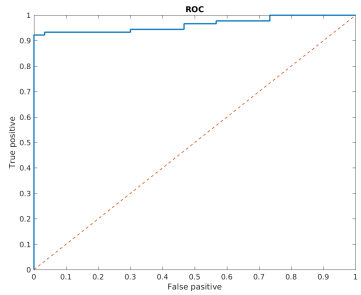

Figure 5.14: ROC curve of a spatial marked image with power equal to 3 and compressed with crf 30

Two studies are presented in this section: the first one concernes the

power of the watermark needed in order to achieve robustness against different levels of compression; the second one focus on youtube, and tries to find the right power to achive robustness in a downloaded video.

Each test has been made with both the ground truth and graph-cuts disparities.

The tables xxs shows how the algorithm manage to find the watermark in a compressed video, in particular its shown if the mark is detected in the left/right view or both images. The first table shows the results when the algorithm is used with the ground truth disparity, the second when using graph cuts.

power	compression level	both	left	right
0.3	1	30	0	0
0.3	15	30	0	0
0.3	25	10	5	0
0.3	30	1	1	0
0.6	1	30	0	0
0.6	15	30	0	0
0.6	25	28	0	0
0.6	30	16	2	0

Table 5.1

In the figures xx-yy its show how the uploading and the subsequential download of a non compressed video on youtube degradates the image.

The tables xxs show how a video uploaded on youtube and subsequentially downloaded can preserve the watermark, respectively when the watermark is iserted with the ground truth disparity and with graph cuts.

power	compression level	both	left	right
0.3	1	30	0	0
0.3	15	29	1	0
0.3	25	11	1	0
0.3	30	2	1	0
0.5	1	30	0	0
0.5	15	30	0	0
0.5	25	24	2	0
0.5	30	9	2	0
0.6	1	30	0	0
0.6	15	30	0	0
0.6	25	26	1	1
0.6	30	15	4	0

Table 5.2

power	both	left	right
0.3	1	0	0
0.6	9	1	0
0.7	12	2	0
0.8	16	0	1

Table 5.3

power	both	left	right
0.3	1	0	0
0.5	6	1	0
0.6	11	0	0

Table 5.4

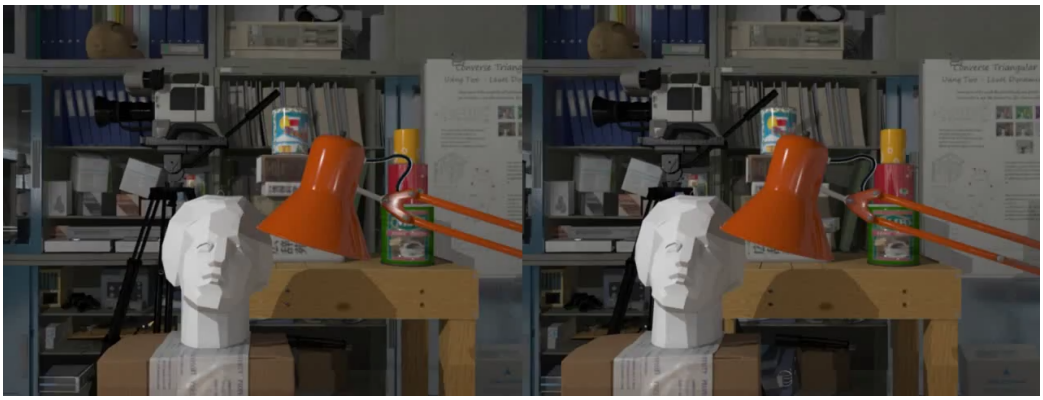

Figure 5.15: stereo image from video uploaded with power equal to 0.3

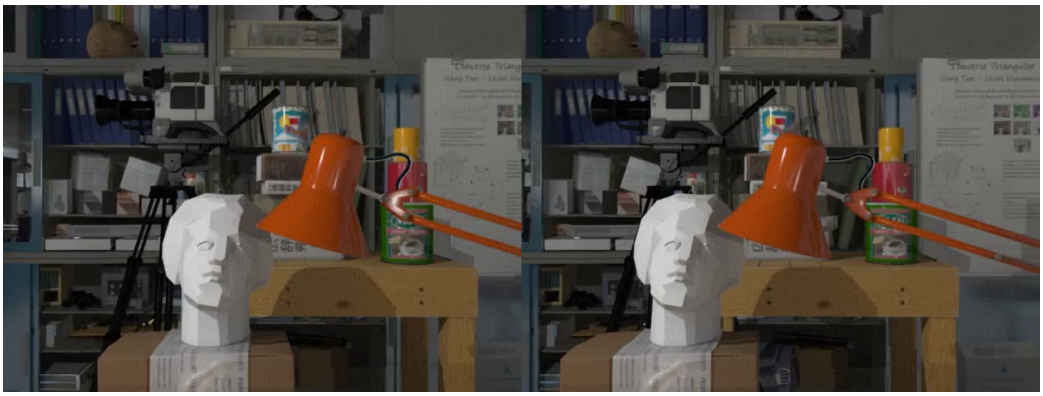

Figure 5.16: stereo image from video uploaded with power equal to 0.6

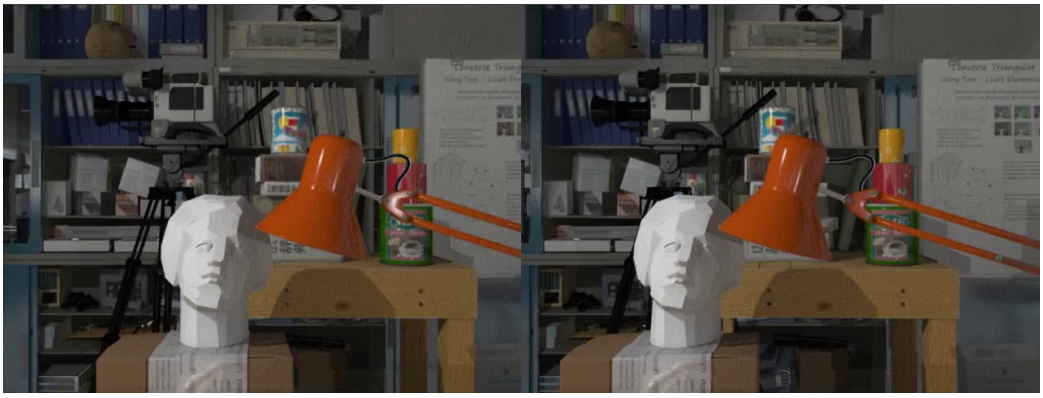

Figure 5.17: stereo image from video uploaded with power equal to 0.7

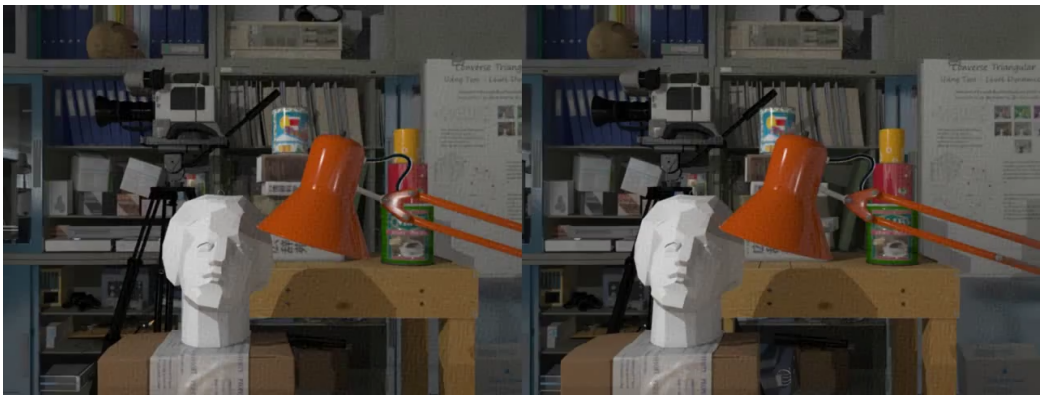

Figure 5.18: stereo image from video uploaded with power equal to 0.8

One can notice that, at a global level, detection statistics gradually degrade with the compression ratio. The embedded watermark becomes hardly detectable at the crudest compression levels even with if embedded with a strong power.

5.2 Robustness to View Synthesis

In a second batch of experiments, we analyzed the impact of virtual view synthesis on the detection performances of our watermarking system. To this end, we generated a number of intermediate synthetic views, equally spaced apart between the left (reference) view and the right one, using ***(nome sw).

The views have been synthetized for both the spatial and frequency method, the result are shown below.

The table contains the results for the frequency marking: the first column is the distance between the left view and the synthetized one, in terms of fraction of the baseline, then its show in how many synthetized images the mark is detected.

Figure 5.19: synthetized view at distance 1/4 of the baseline from the left image

Figure 5.20: synthetized view at distance 1/2 of the baseline from the left image

Figure 5.21: synthetized view at distance 3/4 of the baseline from the left image

position	both	left	right
1/2	30	0	0
1/4	30	0	0
3/4	29	1	0

Table 5.5

The same study is proposed for the spatial marking: from a video marked with additive gaussian noise distribuited with zero mean and unit variance, added with power equal to 1, have been generated three synthetized views for each pair of marked frames, respectively one in the middle and the other two at 1/4 and 3/4 of distance from the left (OMG CHE DISCORSO BRUTTO) .
The ROC curves below show the results for the different intermediate synthetic views.

It can be noted that the watermark is always detected in the synthetized views, we can therefore expect the synthetized views to behave like the other against compression.

5.3 Transparency

Chapter 6

Conclusions

Bibliography

[1] Vladimir Kolmogorov, Pascal Monasse, and Pauline Tan, Kolmogorov and Zabih's Graph Cuts Stereo Matching Algorithm, Image Processing On Line, 4 (2014), pp. 220–251. http://dx.doi.org/10.5201/ipol.2014.97

[2] Hewage, Chaminda TER, and Maria G.Martini. "Edges-based reduced-reference quality metric for 3D video compression and transmission." Selected Topics in Signal Processing, IEEE Journal of 6.5 (2012): 471-482.

[3] Faridul, Hasan Sheikh, Gwenaël Doërr, and Séverine Baudry. "Disparity estimation and disparity-coherent watermarking." IST/SPIE Electronic Imaging. International Society for Optics and Photonics, 2015.

[4] L. Scharf, Statistical Signal Processing: detection, estimation, and time series analysis, Add. Wesley, 1991.

[5] Lens Blur in the new Google Camera app
`http://googleresearch.blogspot.it/2014/04/lens-blur-in-new-google-camera-app.html`